Supporting Information for

Nanoscale Metal-Organic Frameworks for Ratiometric Oxygen Sensing in Live Cells

Ruoyu Xu,[†,1] Youfu Wang,[†,1,2] Xiaopin Duan,[1] Kuangda Lu,[1] Daniel Micheroni,[1] Aiguo Hu,[2] and Wenbin Lin[*,1]

[1]Department of Chemistry, University of Chicago, 929 E 57th St, Chicago, IL 60637, USA

[2]Shanghai Key Laboratory of Advanced Polymeric Materials, School of Materials Science and Engineering, East China University of Science and Technology, Shanghai 200237, China

[†]R.X and Y.W. contributed equally.

Table of Contents

1. Materials and Cell Lines

All compounds were purchased from Sigma-Aldrich or Fisher (USA) and used as received. CT26 cells (mouse colon carcinoma) were purchased from American Type Culture Collection (ATCC, Rockville, MD, USA) and cultured in RPMI 1640 medium containing 10% fetal bovine serum (FBS, Gibco, Grand Island, NY, USA).

2. Synthesis and Characterization of Ligands and UiO MOFs

2.1. Synthesis of H_2QPDC-NH_2 and H_2DBP-Pt

1). Synthesis of H_2QPDC-NH_2

Amino-quaterphenyldicarboxylic acid (H_2QPDC-NH_2) was synthesized as shown in Scheme S1.

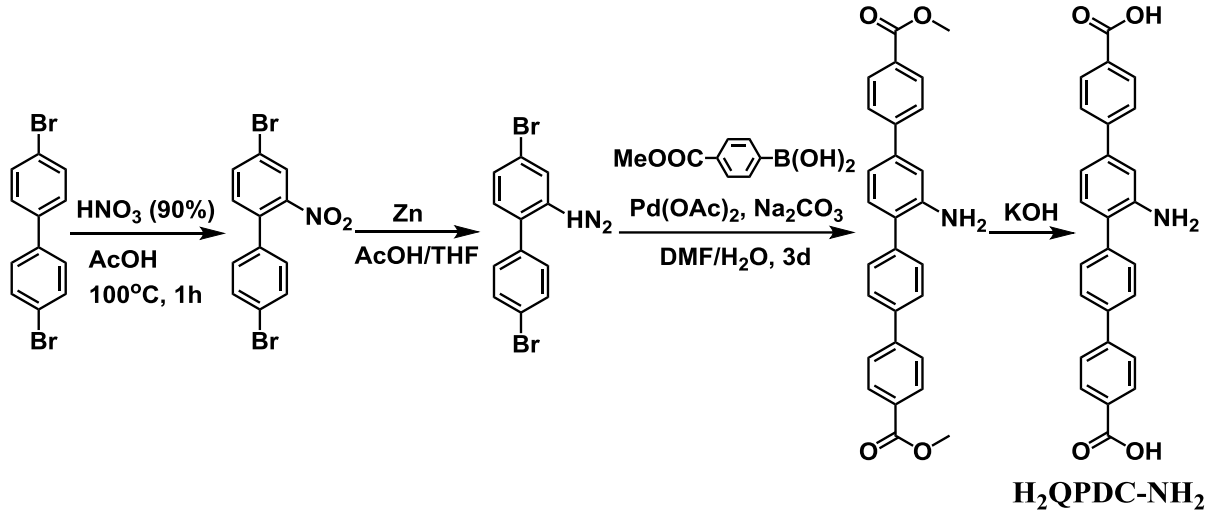

Scheme S1. Synthesis of H_2QPDC-NH_2.

2-Amino-4,4'-dibromobiphenyl. To a solution of 2-nitro-4,4'-dibromobiphenyl (5.00 g, 14.0 mmol) in THF (40 mL) was added Zn powder (9.16 g, 140 mmol) and acetic acid (8.01 mL, 140 mmol). The reaction mixture was stirred at RT for 24 h. CH_2Cl_2 (100 mL) was added, and the Zn powder was removed by filtration through celite. The filtrate was washed with water (2×25 mL), Na_2CO_3 (satd) (25 mL), and brine (25 mL). The organic extract was dried over $MgSO_4$ and filtered. After evaporation of the solvent, the residue was subjected to flash column chromatography on silica gel (10:90 CH_2Cl_2/hexanes to 50:50 CH_2Cl_2/hexanes as eluent) affording 2-amino-4,4'-dibromobiphenyl (3.78 g, 11.6 mmol, 82.5% yield) as a colorless solid. ^{1}H NMR (500 MHz, $CDCl_3$): δ 7.57 (d, *J* = 6.5 *Hz*, 2H), 7.28 (d, *J* = 6.5 *Hz*, 2 H), 6.93-6.91 (m, 3H), 3.87 (bs, 2H); ^{13}C NMR (125 MHz, $CDCl_3$): δ 137.30, 132.15, 131.55, 130.65, 125.20, 122.42, 121.72, 121.67, 118.28; ESI-MS: calcd. for $[M]^+$ 324.9; found 324.9.

Methyl Amino-quaterphenyldicarboxylic ester (Me_2QPDC-NH_2). 4,4'-dibromo-2-amino-1,1'-biphenyl (3.00 g, 9.17 mmol) and methyl-4-carboxylphenyl boronic acid (4.95 g, 27.5 mmol) were

charged to a 2-neck RB flask fitted with a reflux condenser, and then DMF (82.8 mL) was added. The solution was degassed by freeze-pump-thaw twice, and palladium(II) acetate (103 mg, 0.458 mmol) was added. The solution was degassed further for 30 minutes by sparging N_2. Na_2CO_3•H_2O (4.65 g, 33.6 mmol) dissolved in deionized water (50 mL) then degassed by freeze-pump-thaw (5x) was added under N_2. The reaction mixture was then heated under N_2 at 70 ˚C for 72 h. The solution was cooled to room temperature, and the crude reaction mixture was concentrated by rotary evaporation. The remaining solid was then added a 1:1 mixture of $CHCl_3$/H_2O (250 mL total volume) and stirred for 1 hour. The organic layer was isolated with a separatory funnel, and the aqueous was further extracted with chloroform (3×100 mL). The combined organic extracts were dried with $MgSO_4$, and the volatiles were removed in vacuo. The remaining solids were purified by column chromatography using chloroform as the eluent, affording Me_2QPDC-NH_2 as a pale yellow solid (1.78 g, 4.07 mmol, 44% yield). ^{1}H NMR (500 MHz, $CDCl_3$): δ 8.10 (dd, *J* = 10.5, 9.5 *Hz*, 4H), 7.94 (d, *J* = 8.0 *Hz*, 2 H), 7.90 (d, *J* = 8.5 *Hz*, 2H), 7.82 (d, *J* = 8.5 *Hz*, 2H), 7.66 (d, *J* = 8.5 *Hz*, 2H), 7.23 (d, *J* = 8.0 *Hz*, 1H), 7.21 (d, *J* = 2.0 *Hz*, 1H), 7.07 (dd, *J* = 1.5, 7.2 *Hz*, 1H), 5.13 (bs, 2H), 3.93 (s, 3H), 3.92 (s, 3H); ESI-MS: calcd. for $[M+H]^+$ 438.2; found 438.1.

Amino-quaterphenyldicarboxylic acid (H_2QPDC-NH_2). A suspension of Me_2QPDC-NH_2 (1.40 g, 3.20 mmol) in THF (220 mL) was heated to 40 ˚C. A solution of KOH (23.3 g, 414 mmol) dissolved in MeOH (80 mL) was then added, and the reaction mixture was stirred at 40 ˚C for 16 h. The suspension was cooled to room temperature, and the resulting precipitate was collected by centrifugation. The solid was washed with dry THF (20 mL) and re-collected by centrifugation. The solid was suspended in THF (20 mL) and trifluoroacetic acid (5 mL) was slowly added and stirred for 1.5 h at room temperature. H_2O (15 mL) was then added, and the yellow solid was isolated by centrifugation. The collected yellow solid was first washed with THF (10 mL), then Et_2O (10 mL), then dried in vacuo to obtain H_2QPDC-NH_2 as a yellow powder (1.31 g, 2.75 mmol, 85.9% yield). ^{1}H NMR (500 MHz, DMSO-d_6): δ 13.0 (bs, 2H), 8.10-8.06 (m, 4H), 7.89 (dd, *J* = 12.5, 11 *Hz*, 4H), 7.78 (d, *J* = 8.5 *Hz*, 2H), 7.65 (d, *J* = 8.0 *Hz*, 2H), 7.21-7.20 (m, 2H), 7.05 (d, *J* = 7.5 *Hz*, 1H), 5.16 (bs, 2H); ^{13}C NMR (125 MHz, $CDCl_3$): δ 167.66, 167.63, 146.23, 145.11,144.39, 139.65, 139.57, 137.87, 131.27, 130.53, 130.42, 130.06, 129.91, 129.72, 127.80, 127.11, 126.94, 125.54, 116.03, 114.17; ESI-MS: calcd. for $[M+H]^+$ 410.1, found 410.0.

2). Synthesis and Characterization of H_2DBP-Pt

Pt(II)-5,15-di(*p*-benzoato)porphyrin (H_2DBP-Pt) was synthesized by refluxing K_2PtCl_4 and 5,15-di(*p*-methyl-benzoato)porphyrin (Me_2DBP) in benzonitrile followed by hydrolysis, as shown in Scheme S2. Me_2DBP was synthesized according to our previous report.[1]

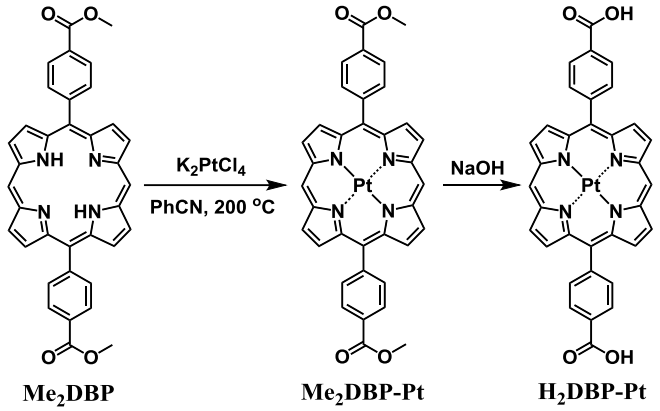

Scheme S2. Synthetic route of H_2DBP-Pt.

Me_2DBP-Pt was prepared by refluxing K_2PtCl_4 (300 mg, 720 μmol) and 5,15-di(*p*-methyl-benzoato)porphyrin (Me_2DBP) (210 mg, 360 μmol) in benzonitrile (130 mL) in a sand bath for 24 h. After cooling to room temperature, benzonitrile was removed under reduced pressure. The crude product was purified by silica gel column chromatography with methylene chloride as eluent to afford a deep red product. Yield: 190 mg, 246 μmol, 68 %. The ^{1}H NMR spectrum of Me_2DBP-Pt is shown in Figure S1. ^{1}H-NMR (500 MHz, Chloroform-D, ppm): δ = 10.21 (s, 2H), 9.26 (d, 4H), 8.90 (d, 4H), 8.48 (d, 4H), 8.31 (d, 4H), 4.14 (s, 6H). ESI-MS for Me_2DBP-Pt ($C_{36}H_{24}N_4O_4Pt$) $[M+H]^+$: calcd. 772.1; found: 772.1.

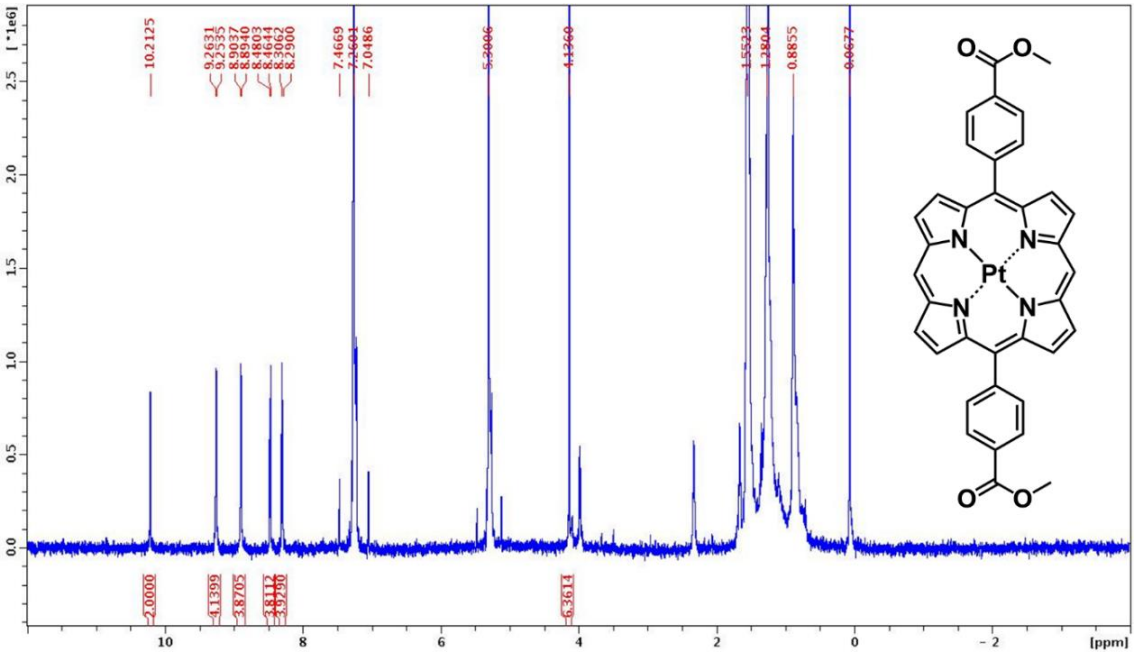

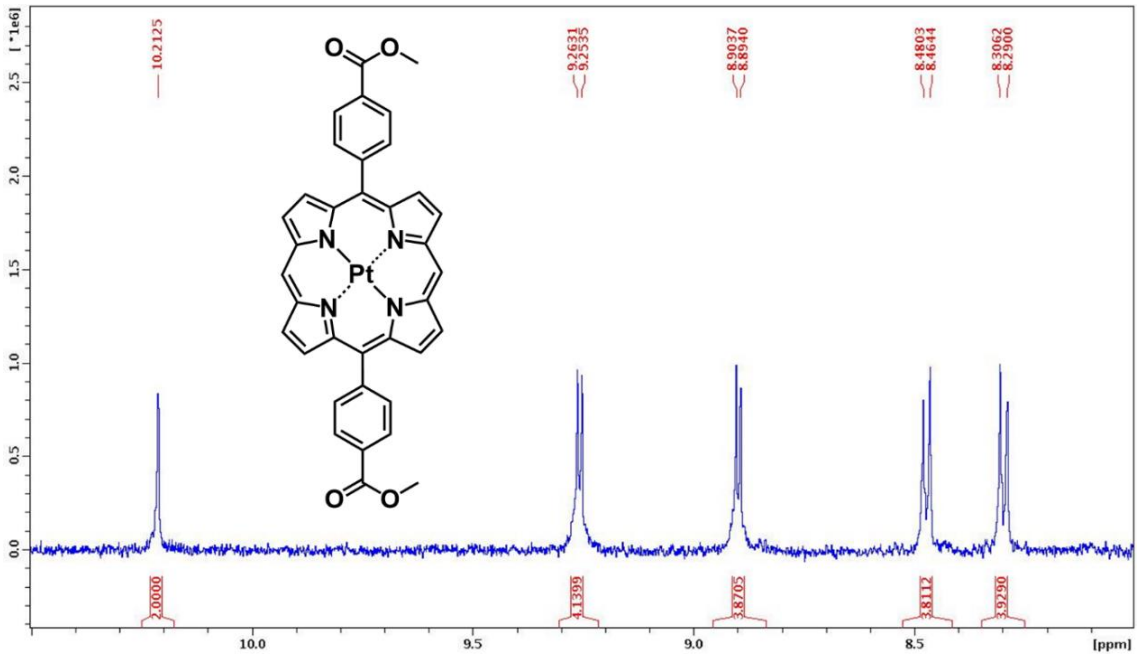

Figure S1. ^{1}H NMR spectrum of Me_2DBP-Pt.

H_2DBP-Pt was prepared by refluxing Me_2DBP-Pt (190 mg, 246 μmol) in a mixture of tetrahydrofuran (THF, 15 mL), methanol (15 mL), and an aqueous solution of potassium hydroxide (5 mL, 2 M) for 12 h. After cooling to room temperature, most of the solvent was removed by rotary evaporation before the solution was acidified to pH < 3 with hydrochloric acid. The red product was obtained by filtration and washed with water and ether and then dried under a vacuum. Yield: 178 mg, 240 μmol, 98 %. The ^{1}H NMR spectrum of H_2DBP-Pt is shown as Figure S2. ^{1}H NMR (500 MHz, DMSO-D_6, ppm): δ =13.35 (s, 2H), 10.60 (s, 2H), 9.54 (d, 4H), 8.90 (d, 4H), 8.42 (d, 4H), 8.36 (d, 4H). ESI-MS for H_2DBP-Pt ($C_{34}H_{20}N_4O_4Pt$) $[M+H]^+$: calcd. 744.1; found: 744.1.

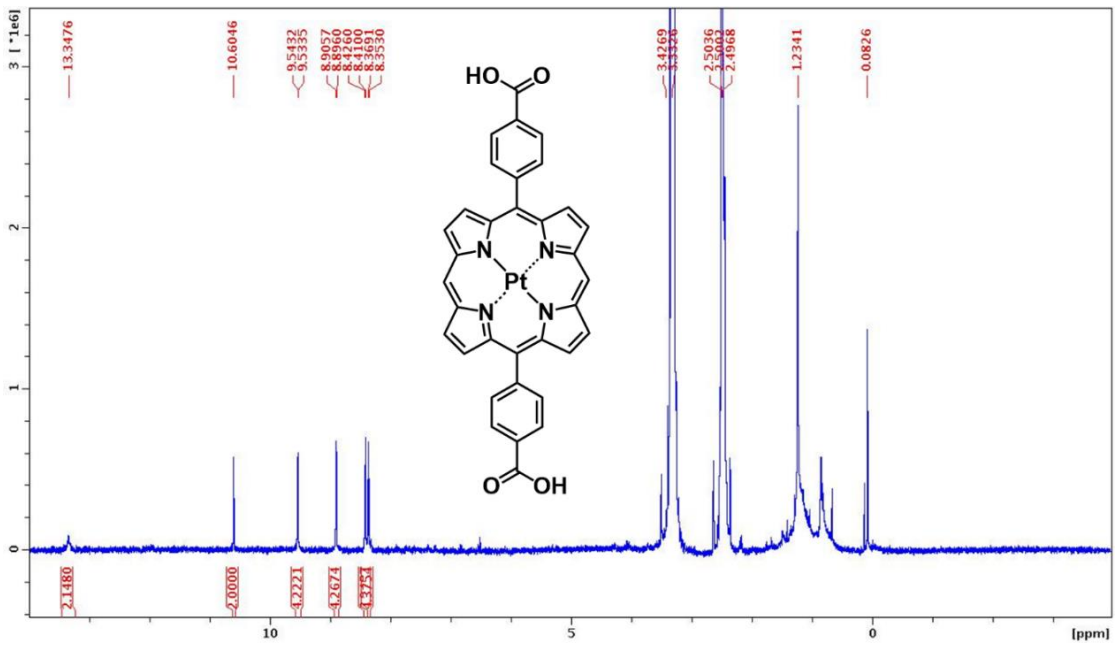

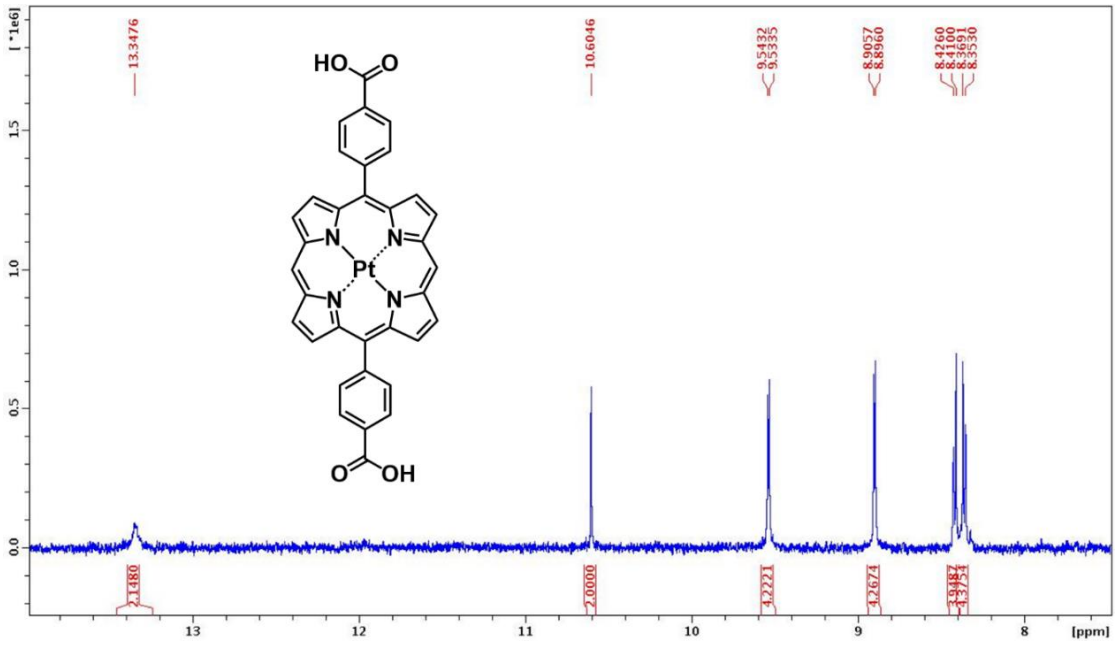

Figure S2. ^{1}H NMR spectrum of H_2DBP-Pt.

2.2. Synthesis of Mixed-ligand UiO NMOF (M-UiO)

The M-UiO NMOF was synthesized by a solvothermal method. Briefly, H_2QPDC-NH_2 (20.5 mg, 50 μmol) and H_2DBP-Pt (7.44 mg, 10 μmol) were mixed with 1 mL AcOH and 19 mL dimethylformamide (DMF) solution of $HfCl_4$ (19.2 mg, 60 μmol), and the mixture was kept in an 80 °C oven for 4 days. The product was collected by centrifugation and washed with DMF and ethanol.

Transmission electron microscopy (TEM, Tecnai F30 and Tecnai Spirit, FEI, USA) was utilized to confirm the morphology of the M-UiO NMOF. The particle size of M-UiO was determined by dynamic light scattering (DLS, Nano-ZS, Malvern, UK) (Figure S3).

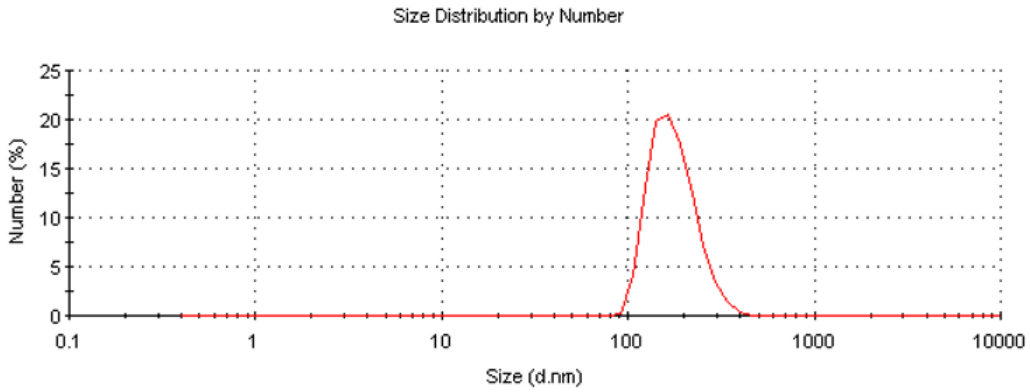

Figure S3. DLS measurement showing the particle size of M-UiO NMOF. The number-averaged diameter of M-UiO is 177.8 nm with PDI = 0.064.

The UV-vis absorption spectrum (UV-2401PC, Shimadzu, Japan) of M-UiO NMOF is shown in Figure S4. The two characteristic Q-bands of DBP-Pt indicated that there is negligible platinum leaching during the growth of M-UiO NMOF.

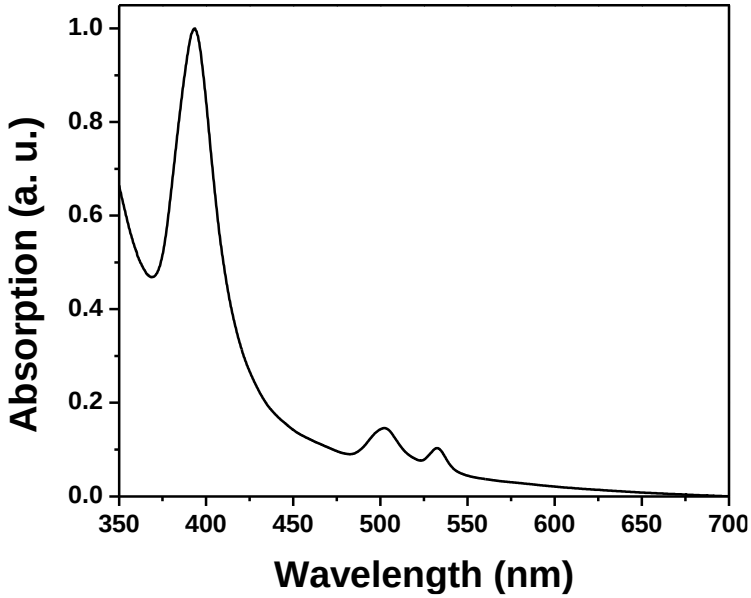

Figure S4. UV-vis absorption spectrum of M-UiO NMOF.

3. Post-Synthesis Modification of M-UiO with RITC

3.1. Photophysical properties of H_2DBP-Pt and RITC

The UV-vis spectra of H_2DBP-Pt and RITC were obtained in DMSO on a spectrometer and shown in Figure S5. The emissions of H_2DBP-Pt and RITC were measured in MeOH on a fluorimeter (RF-5301PC) with excitations of 391 nm and 514 nm, respectively.

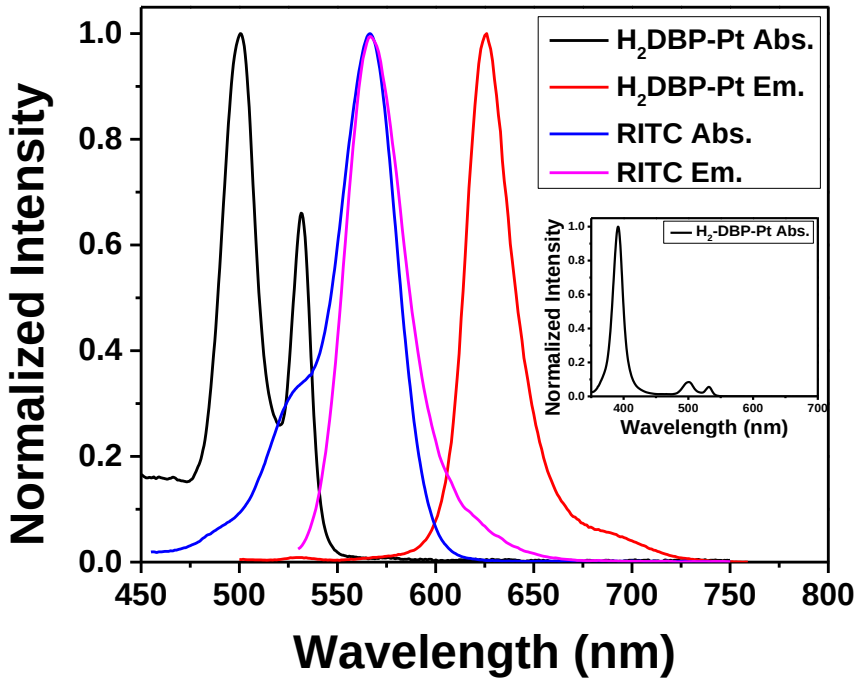

Figure S5. UV-vis absorption (in DMSO) and emission (in MeOH) spectra of H_2DBP-Pt and RITC.

3.2. Synthesis and Characterization of R-UiO

A methanol solution of Rhodamine-B-Isothiocyanate (RITC, 1 mM) was added to 2.0 mg of M-UiO NMOF suspended in 0.5 mL methanol. The mixture was stirred gently at room temperature in the dark for 3 h to afford Rhodamine-B-conjugated M-UiO NMOFs (R-UiO). 40 μL/150 μL RITC solution were used to afford R-UiO-1/R-UiO-2. The product was collected by centrifugation and washed with ethanol, yielding R-UiO as a red powder. R-UiO was saved in ethanol as a stock solution for further use.

The conjugation of RITC with the ligand (H_2QPDC-NH_2) in R-UiO was confirmed by mass spectrometry (Agilent 1100 LC/MSD with ESI and APCI ion sources). For mass spectrometric analysis, R-UiO in ethanol was digested with HF solution in methanol. The sample was delivered with methanol. RITC-attached ligands (R-QPDC, exact mass = 909) were observed as shown in Figure S6.

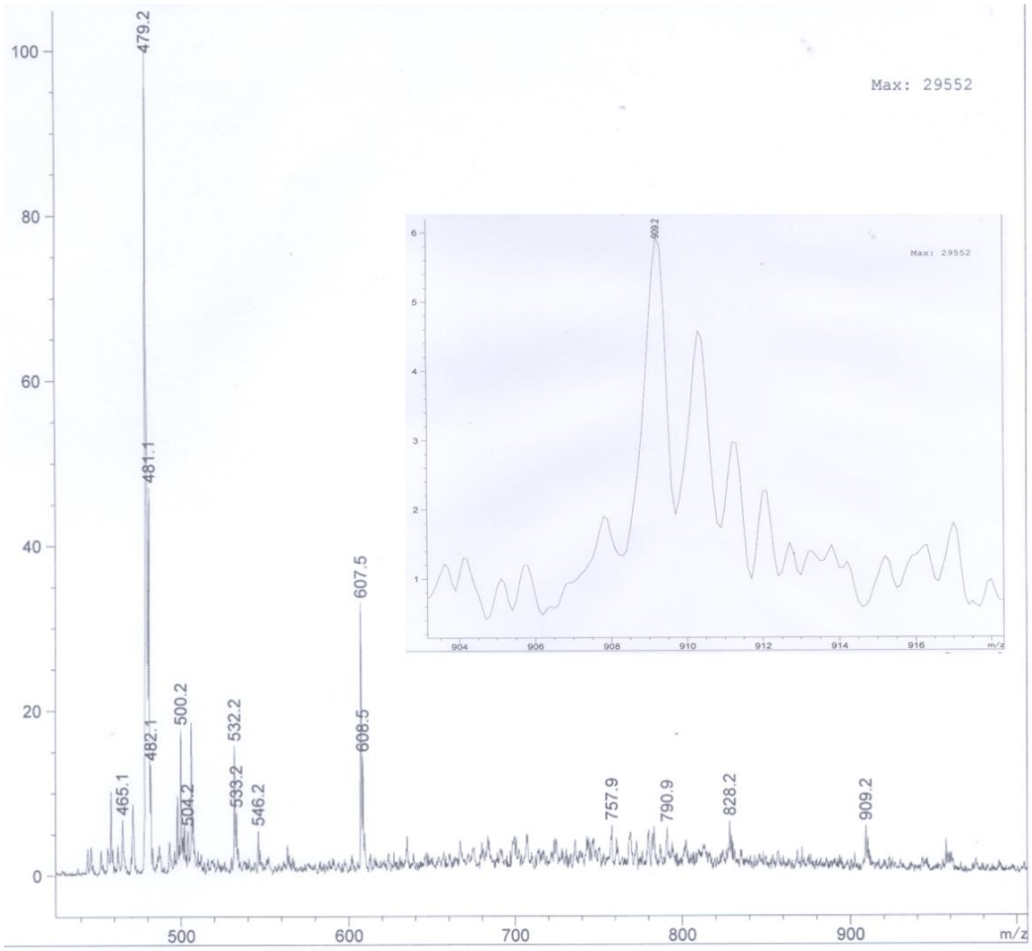

Figure S6. Mass spectrum of digested R-UiO. R-UiO was digested with HF in methanol. The sample was delivered with methanol.

The morphology of R-UiO was evaluated by TEM and the particle size was determined by DLS (Figure S7). The size of R-UiO is slightly larger than the UiO NMOF, as determined by DLS.

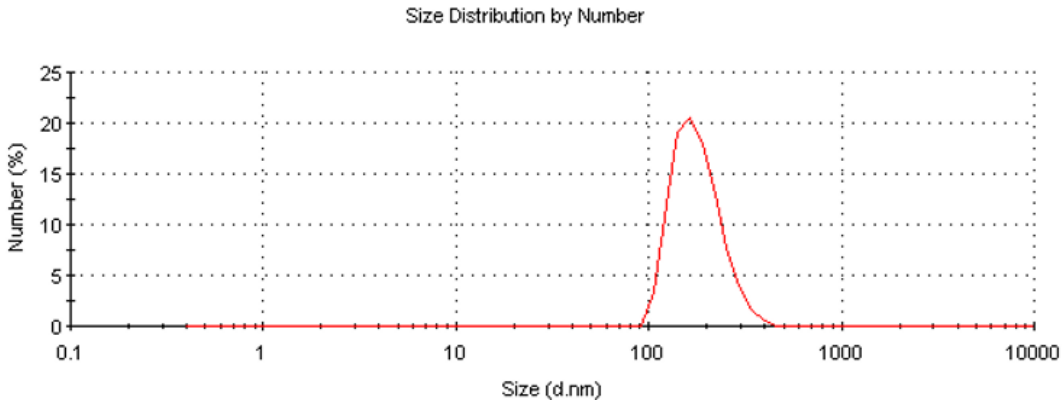

Figure S7. DLS measurement showing the particle size of R-UiO. The number-averaged diameter of R-UiO is 181.1 nm with PDI = 0.079.

3.3. Quantum Yields of R-UiOs in HBSS

The quantum yields of R-UiO-1 and R-UiO-2 were measured in HBSS using Rhodamine-B as standard (QY = 0.31 in water excited at 514 nm).[2] The quantum yield of the R-UiO-1 and R-UiO-2 in HBSS was calculated according to the following equation:

$$\Phi = \Phi_r * \frac{A_r}{I_r} * \frac{I}{A} * \frac{{n_r}^2}{n^2}$$

where ϕ is the quantum yield, I is the measured integrated emission intensity, n is the refractive index (1.333 for water), and A is the optical density. The subscript "r" refers to the reference fluorophore of known quantum yield. In order to minimize re-absorption effects, the absorbencies in the 10 mm fluorescence cuvette were kept under 0.1 at the related excitation wavelengths.

The quantum yields of R-UiO-1 and R-UiO-2 are 0.08 and 0.15, respectively (excited at 514 nm).

4. Structural Stability of R-UiO in HBSS

4.1. Dye Release

The H_2DBP-Pt and Rhodamine-B released from R-UiO in HBSS was detected by UV-vis spectra of the supernatant. 100 μg R-UiO was incubated in 1mL HBSS. After incubating for 1 h, 2 h, 4 h, and 24 h, the suspension was subjected to centrifugation at 13,000 rpm for 15 min. 0.6 mL of the supernatant was collected and another 0.6 mL of fresh HBSS was added. The supernatant was diluted to 1.2 mL and used for UV-vis spectra measurement (Figure S8). The result showed negligible dye release after incubation in HBSS for 24h.

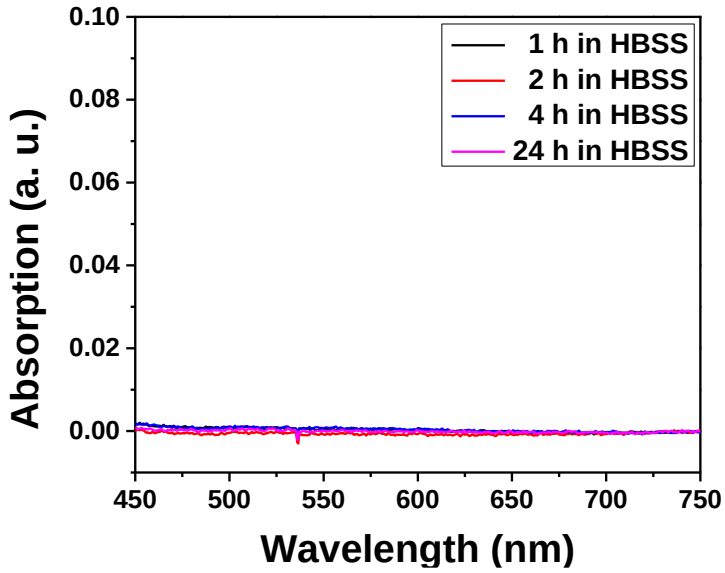

Figure S8. Release profile of H_2DBP-Pt and Rhodamine B from R-UiO in HBSS after different incubation times.

4.2. Structural Stability of R-UiO in HBSS

R-UiO was incubated in HBSS at room temperature for 1 h, 4 h, and 24 h. The morphology of HBSS-treated R-UiO was observed by TEM and shown in Figure S9 and S10. The morphology and size of these NMOFs were similar to the as-synthesized R-UiO, which indicated the structural stability of the R-UiO NMOF system.

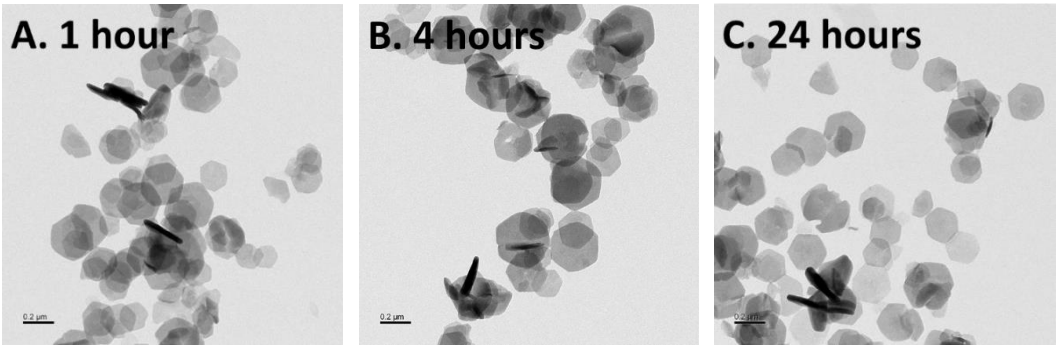

Figure S9. TEM images of R-UiO incubated with HBSS for 1 h, 4 h, and 24 h.

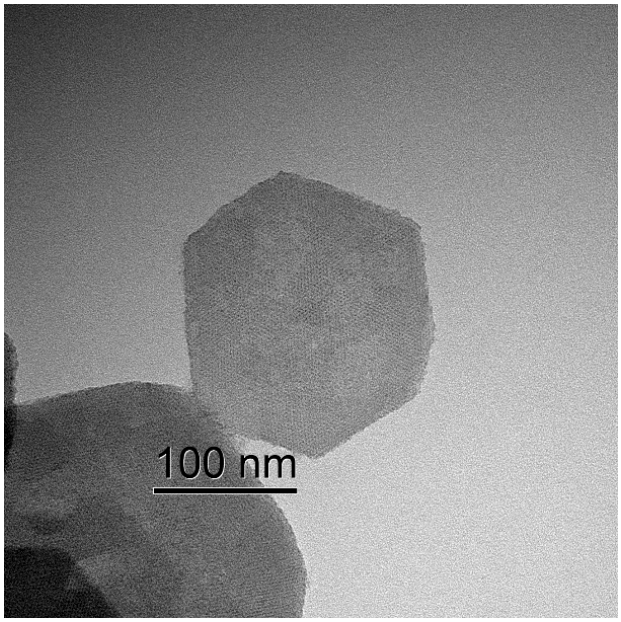

Figure S10. High-resolution TEM image of R-UiO after incubation in HBSS for 24 h.

The powder X-ray diffraction (PXRD) patterns of these NMOF samples were collected on a Bruker D8 Venture, dual microsource (Cu and Mo) diffractometer with a CMOS detector. Cu Kα radiation was used. The PXRD patterns were processed with the APEX 2 package using a PILOT plug-in. The PXRD patterns of R-UiO after incubating with HBSS for 12 h and 24 h were collected and compared with those of the original UiO NMOF and R-UiO before HBSS treatment.

The emission spectrum of R-UiO-1 in MeOH excited at 391 nm was shown in Figure S11.

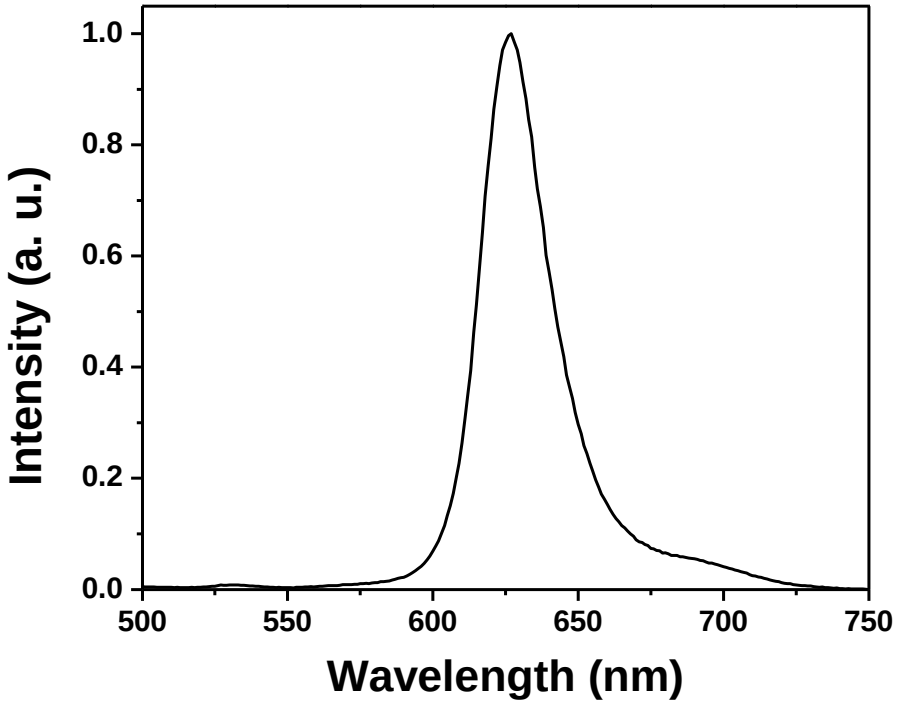

Figure S11. The emission of R-UiO-1 in methanol (excited at 391 nm).

5. H_2DBP-Pt and RITC Loading Quantification

The H_2DBP-Pt and RITC loadings in R-UiO were determined by ICP-MS (Agilent 7700X) and the absorption of the digested R-UiO, respectively.

To test platinum loading, 150 μL R-UiO (~1 mg/mL) suspension in ethanol was added into 6 mL HNO_3/HF/HCl (18:1:1 v/v/v), which was then digested at 170 °C for 20 min (MARS 6, OneTouch) to ensure complete porphyrin digestion. The resulting digestion solution was diluted with water. Hf and Pt concentration was then obtained by ICP-MS.

For the quantification of Rhodamine-B loading, we tested the UV-vis spectra of RITC under different concentrations as shown in Figure S12A and obtained the standard curve (Figure S12B). We chose the absorption peak of Rhodamine-B-NCS (566 nm) to quantify the loading of Rhodamine-B.

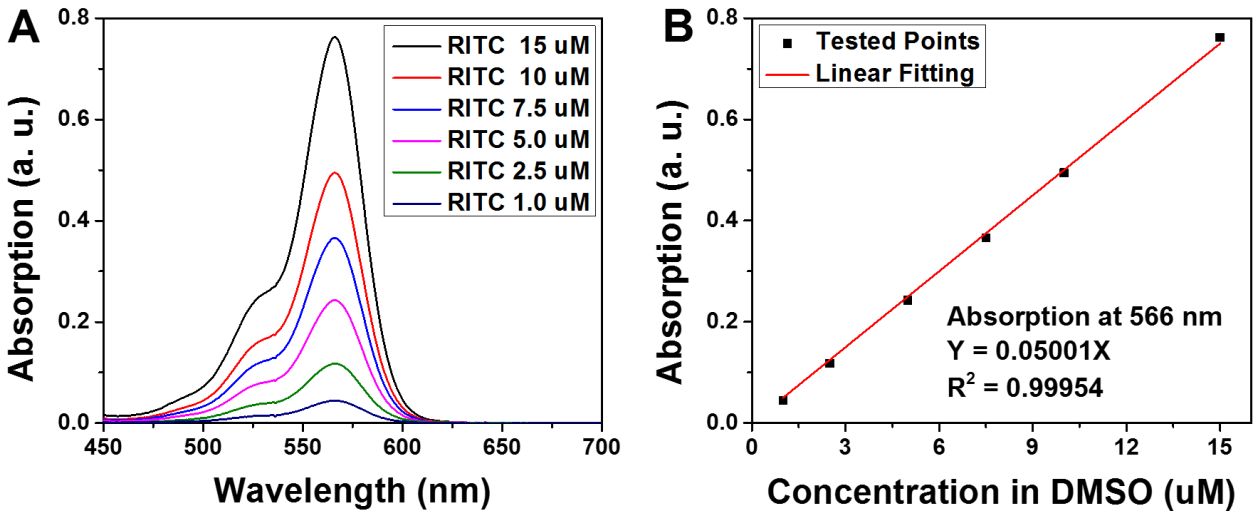

Figure S12. (A) UV-vis absorption spectra of RITC at different concentrations in DMSO and (B) the relationship between the absorption at 566 nm and the concentration.

150 μg R-UiO-1 suspension in 1.5 mL DMSO was digested by adding 4 μL HF. The UV-vis absorption of digested R-UiO-1 in DMSO was presented as Figure S13. The loadings of RITC in R-UiO-1 was determined to be 0.6% mol. Similarly, RITC loading in R-UiO-2 was 1.6% mol.

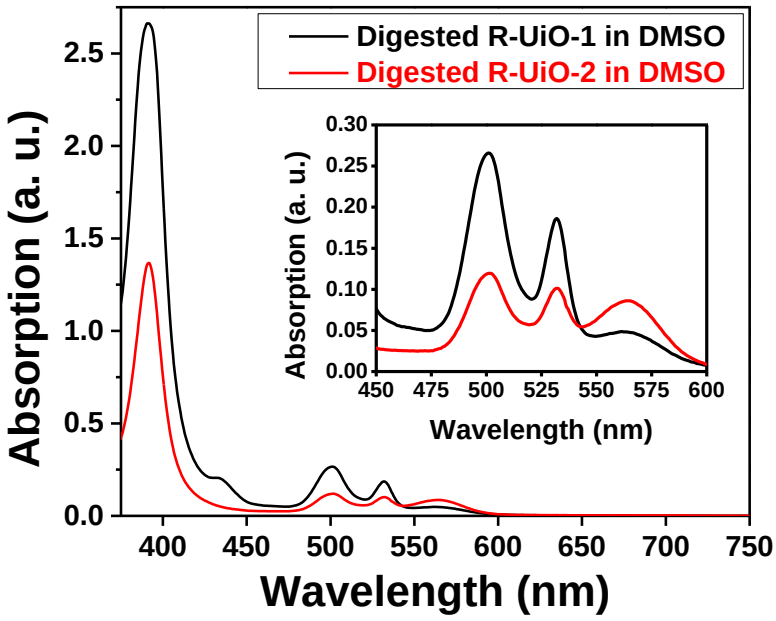

Figure S13. Absorption spectra of digested R-UiO in DMSO.

6. Ratiometric Luminescence Response to *Po*$_2$ by Fluorimetry

Emission spectra of R-UiO-1 and R-UiO-2 in HBSS under different *Po*$_2$ were obtained on a fluorimeter (RF-5301PC). A cuvette containing 3 mL R-UiO-1 or R-UiO-2 (10 μg/mL) suspension

was placed in a glove box. The oxygen concentration in the glove box was adjusted by controlling the flow rate of air and nitrogen, and monitored by a commercial oxygen sensor (YSI ProODO 626279). The R-UiO-1 or R-UiO-2 suspension was bubbled with pipette for 5 min to reach equilibrium. The cuvette was then capped and subjected to emission measurements (Figure S14 and S15). It is worth noting that when RITC loading is high (R-UiO-2), the Rhodamine fluorescence peak has non-negligible overlap with DBP-Pt phosphorescence peak, so the R_I^0/R_I will deviate from Stern-Volmer relation (Figure S15B is different from Figure S14B). This spectral overlap may also contribute to the non-linear part of Figure 14B under high oxygen pressure (in the 80-160 mmHg range).

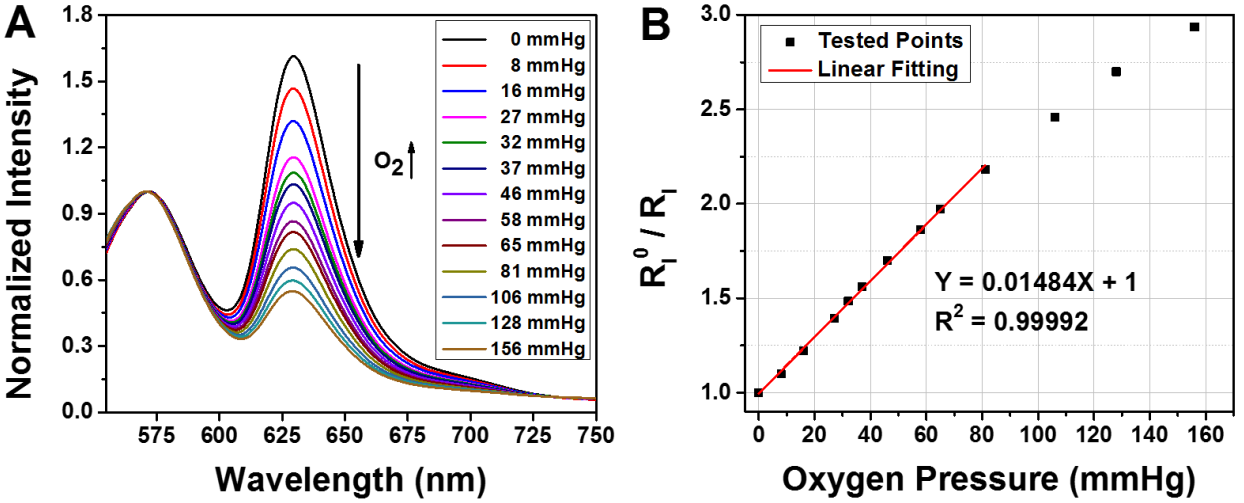

Figure S14. (A) Luminescence spectra of R-UiO-1 under different oxygen partial pressures and (B) R_I^0/R_I as function of P_{O_2} ranging from 0 mmHg to 160 mmHg.

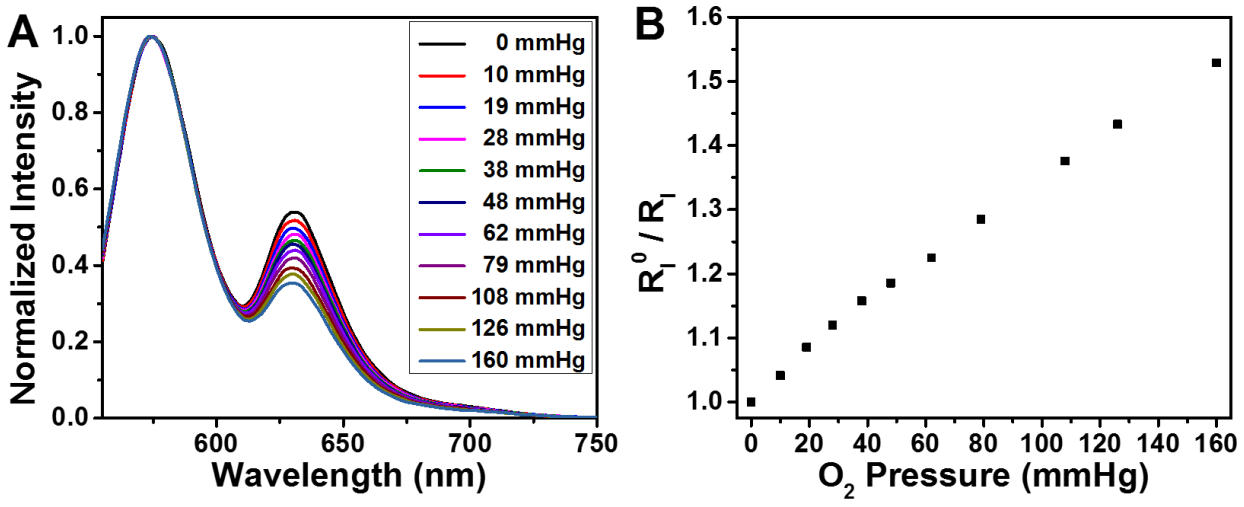

Figure S15. (A) Luminescence spectra of R-UiO-2 under different oxygen partial pressures and (B) R_I^0/R_I as function of P_{O_2} ranging from 0 mmHg to 160 mmHg.

7. Lifetime Response to P_{O_2}

The phosphorescence decay of R-UiO-1 in HBSS under different oxygen concentrations was measured with ChromsBH lifetime fluorimeter (ISS, Inc.). A 405 nm laser was used as the excitation source, and time-lapse 641±37 nm emission intensity was monitored on microsecond scale. A capped cuvette was used to hold the sample, and the sample preparation was similar to that in Part 6. The phosphorescence decay curves were fitted by exponential decay.

We also measure the phosphorescence lifetime of ligand H_2DBP-Pt and R-UiO-2 in methanol under nitrogen as shown in Figure S16. The lifetimes of H_2DBP-Pt and R-UiO-2 are 50.5 μs and 48.7 μs under nitrogen, respectively. Their similar lifetimes further support a negligible energy transfer from Pt-DBP to Rhodamine in R-UiO.

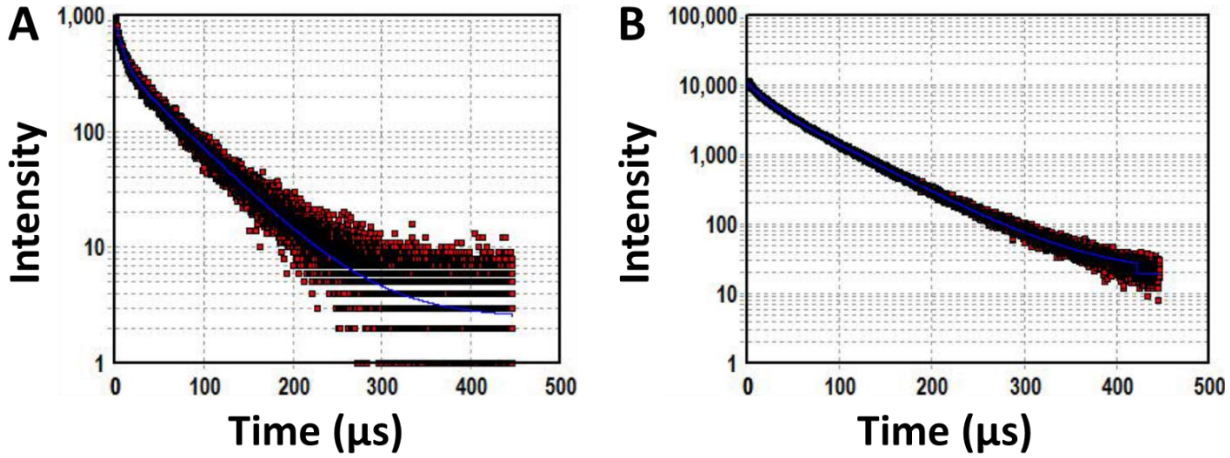

Figure S16. Lifetimes of H_2DBP-Pt (A) and R-UiO-2 (B) in methanol under nitrogen.

8. Ratiometric Luminescence Response to P_{O_2} by CLSM Imaging

The phosphorescence/fluorescence responses to P_{O_2} ranging from 0 mmHg to 160 mmHg of R-UiO-2 in HBSS solution were evaluated by confocal laser scanning microscopy (CLSM, Leica SP5 II, Integrated Microscopy Core Facility at the University of Chicago). 15 μL of R-UiO-2 (1 mg/mL) was dispersed in 1 mL HBSS and transferred to glove box at a preset oxygen partial pressure. The suspension was bubbled for 5 min to reach equilibrium and added to a glass-bottom petri dish (No. 1.5, uncoated glass, MatTek Corporation), which was covered with another inverted petri dish and sealed with parafilm. The sample was then observed under confocal microscope.

Images were collected using Leica SP5 II microscope equipped with 100X, 1.4 oil objective, PMT detector, and transmitted light detector with differential interference contrast (DIC). A 514 nm laser was used as the excitation source. 540-580 nm and 620-660 nm luminescence signals were collected in two different channels. The laser scanning frequency was set to 8 Hz with line scan mode (line average = 1). Images were obtained in the format of 256×256 pixel.[1] The intensity ratio of R-UiO-2 in the two channels were analyzed by ImageJ (Figure S17). 3-8 samples were tested under each condition to give the standard deviation of P_{O_2}. The I_P/I_F - P_{O_2} relation was fitted with the following formula:

$$y = \frac{I_P}{I_F} = \frac{kP_{O_2}+b}{P_{O_2}+c} \qquad \text{(Formula S1)}$$

where y is the intensity ratio of phosphorescence to fluorescence, k, b and c are fitting parameters. The fitted equation is thus derived as:

$$y = \frac{1.544P_{O_2}+398.8}{P_{O_2}+71.77} \quad R^2 = 0.993\ . \qquad \text{(Formula S2)}$$

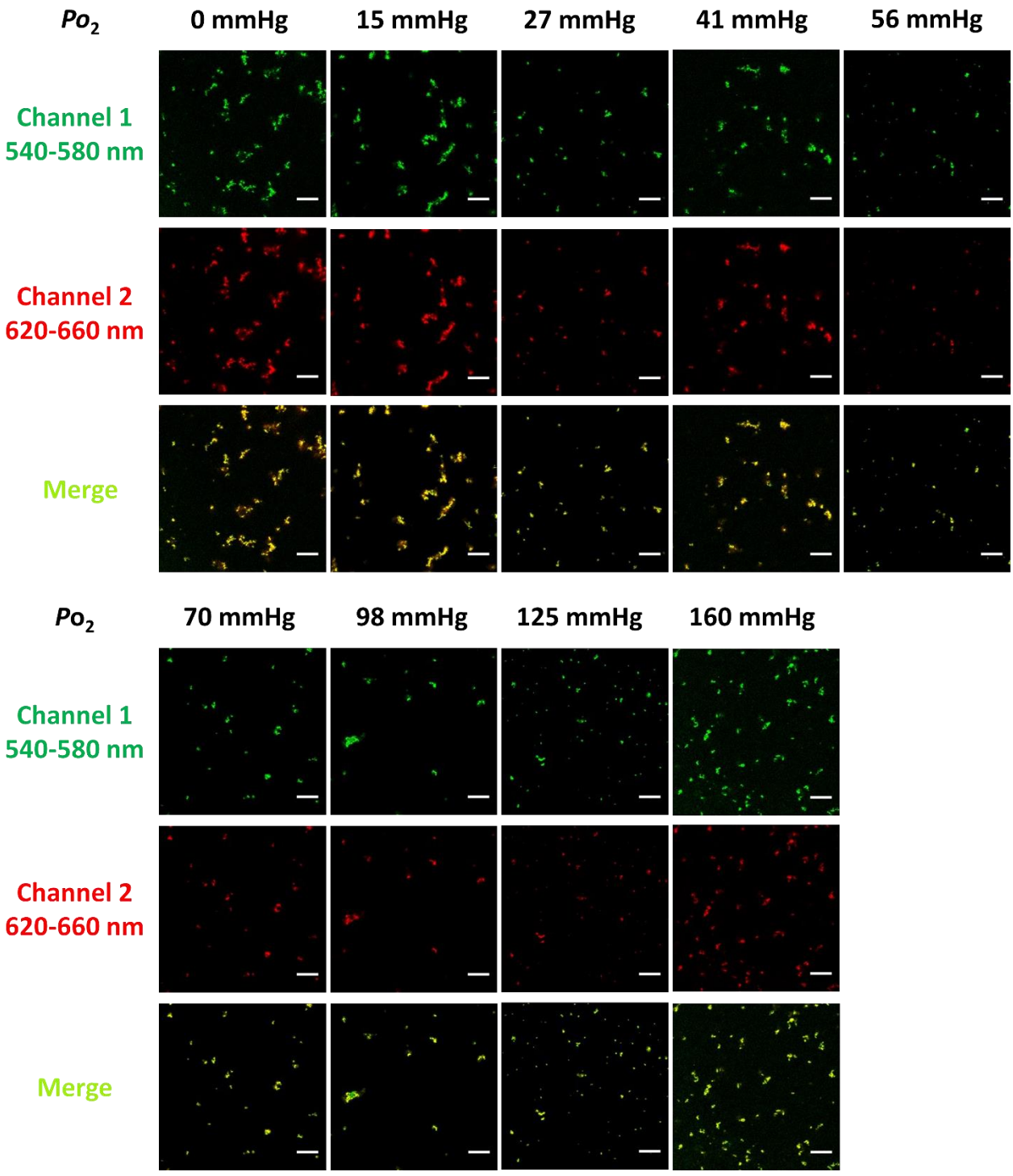

Figure S17. Images of R-UiO-2 dispersed in HBSS with a series of Po_2 acquired by CLSM using 514 nm excitation, and two-channel collection. Bar: 10 μm.

9. Cytotoxicity and Cellular Uptake of R-UiO in CT26 Cells

9.1 Cytotoxicity of R-UiO in CT26 Cells

CT26 cells were seeded on a 96-well plate at a density of 2×10^3 cells per well. After overnight incubation, the cells were treated with different concentrations of R-UiO-2 for 72 h. At the end of the incubation period, cell viability was measured by (3-(4,5-dimethylthiazol-2-yl)-5-(3-carboxymethoxyphenyl)-2-(4-sulfophenyl)-2H-tetrazolium) (MTS) assay (Promega, Madison, WI) according to the manufacturer's instructions.

R-UiO-2 showed low cytotoxicity on CT26 cells with over 90% cell viability at concentration lower than 50 μg/mL (Figure S18). The concentration used for cellular uptake and imaging is 30 μg/mL, less than 50 μg/mL. In addition, the cells were only incubated with R-UiO-2 for 2 h for cellular uptake and imaging, so the cells should be on good condition during the experiments.

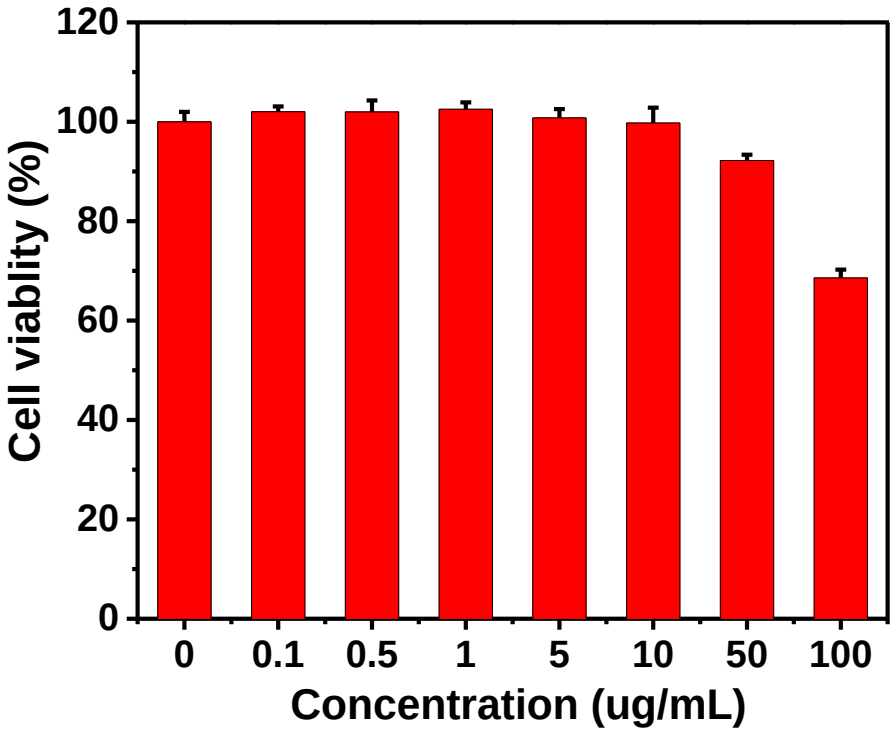

Figure S18. Cytotoxicity of R-UiO-2 in CT26 cells.

9.2 Cellular Uptake of R-UiO in CT26 Cells

CT26 cells were seeded on a 6-well plate at 1×10^6 cells per well and cultured for 24 h. 30 μL R-UiO-2 (2 mg/mL) were added to each well. After incubation for 10 min, 20 min, 30 min, 60 min,

and 120 min, cell media were discarded. The cells were washed with HBSS three times, and counted with hemocytometer. The cells were then centrifuged at 3,000 rpm for 5 min, and the cell pellet was digested with 100 μL HNO_3/HF (9:1 v/v). After 24 h, the digestion was diluted with water and subjected to ICP-MS to determine the Hf concentration. Three parallel experiments were conducted for each time point. Results were expressed as the amount of R-UiO-2 calculated from the Hf concentration associated with one cell.

10. Live Cell Image Acquisition and Analysis

CT26 cells were seeded on a glass-bottom petri dish at a density of 1×10^6 cells/well and cultured for 24 h. 30 μL R-UiO-2 (2 mg/mL) was then added and the cells were cultured for another 2 h. The cell media were discarded, and the cells were washed with HBSS three times and sealed in the petri dish under different Po_2 using the method described in Part 8.

Images were collected using Leica SP5 II microscope equipped with 100X, 1.4 oil objective, PMT detector, and transmitted light detector with differential interference contrast (DIC). The laser scanning frequency was set to 8 Hz with line scan mode (line average = 1). Images were obtained in the format of 256×256 pixel.[1] Cells were imaged in three channels to yield three images: (1) exciting at 514 nm and collecting at 540-580 nm; (2) exciting at 514 nm and collecting at 620-660 nm; (3) DIC. (Figure S19) The data were process by ImageJ and the intensity ratio of R-UiO-2 in Channel 1/Channel 2 was obtained. Using the standard curve under CLSM as reference, the oxygen partial pressure can be calculated. 3-8 samples were tested under each condition to give the standard deviation. According to Formula S1,

$$P_{O_2} = \frac{b-cy}{y-k} \qquad \text{(Formula S3)}$$

$$dP_{O_2} = \frac{kc-b}{(y-k)^2} \qquad \text{(Formula S4)}$$

Using the fitting data b = 398.8 mmHg, c = 71.77 mmHg, k = 1.544,

Insert y = 5.29, $dy = 0.12$ into Formula S3 and S4 respectively, we get $P_{O_2} = 5.1$ mmHg, $dP_{O_2} = 2.5$ mmHg;

Similarly, when $\frac{I_P}{I_F} = 4.45 \pm 0.09$, $P_{O_2} = 27.3 \pm 3.1$ mmHg;

when $\frac{I_P}{I_F} = 2.80 \pm 0.06$, $P_{O_2} = 158 \pm 11$ mmHg.

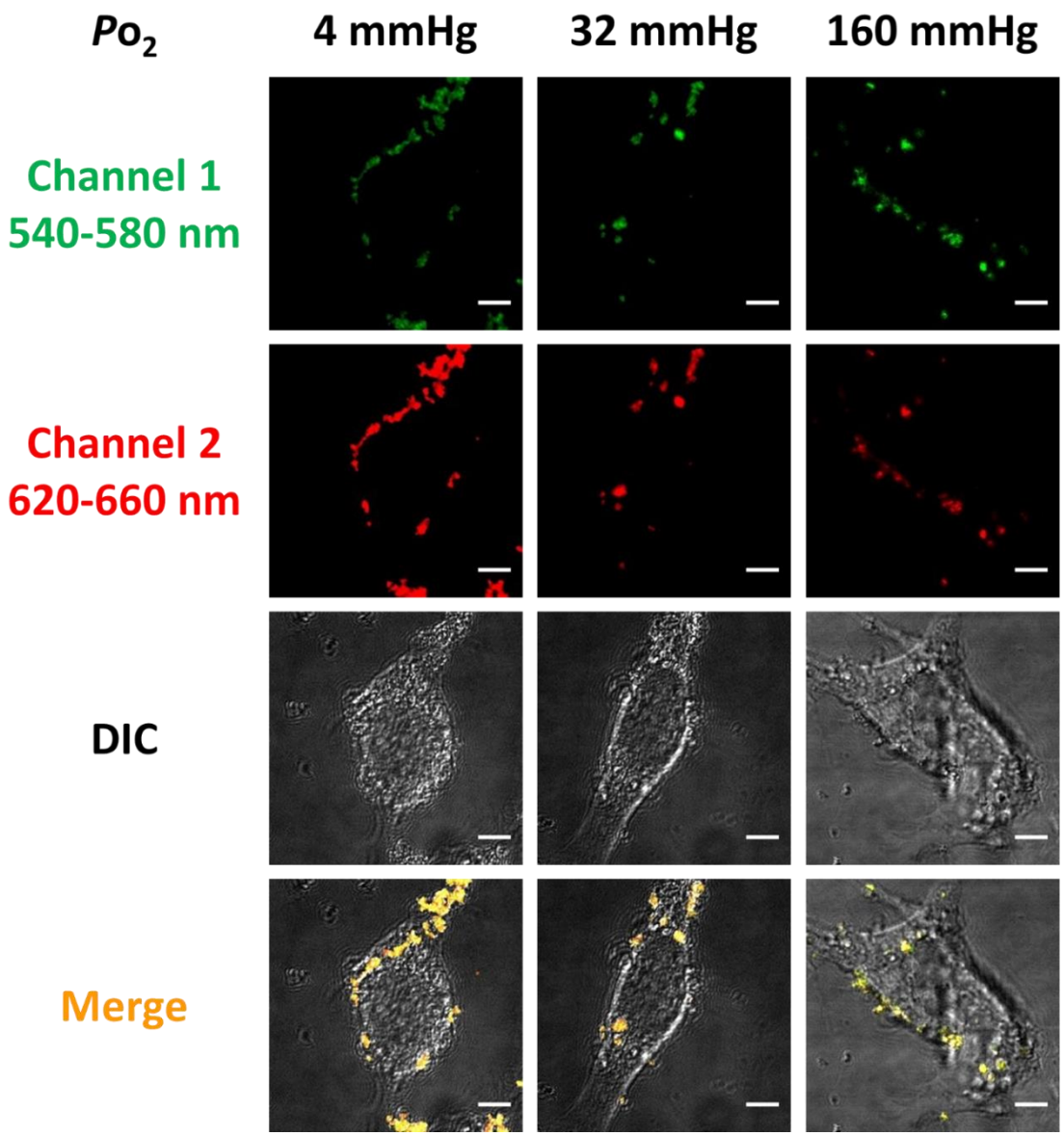

Figure S19. CLSM images of live cells under hypoxia (4 mmHg), normoxia (32 mmHg), and aerated conditions (160 mmHg) after incubation with R-UiO-2. Bar: 5 μm.

11. Photostability of R-UiO

Cellular uptake of R-UiO was performed following the procedure in 9.2 for 2 h. After washing with HBSS three times, the photoluminescence stability of R-UiO-2 in CT26 cells under CLSM in air was measured and shown in Figure S20. The phosphorescence/fluorescence intensity ratio of R-UiO remains stable 4 hours after cellular uptake.

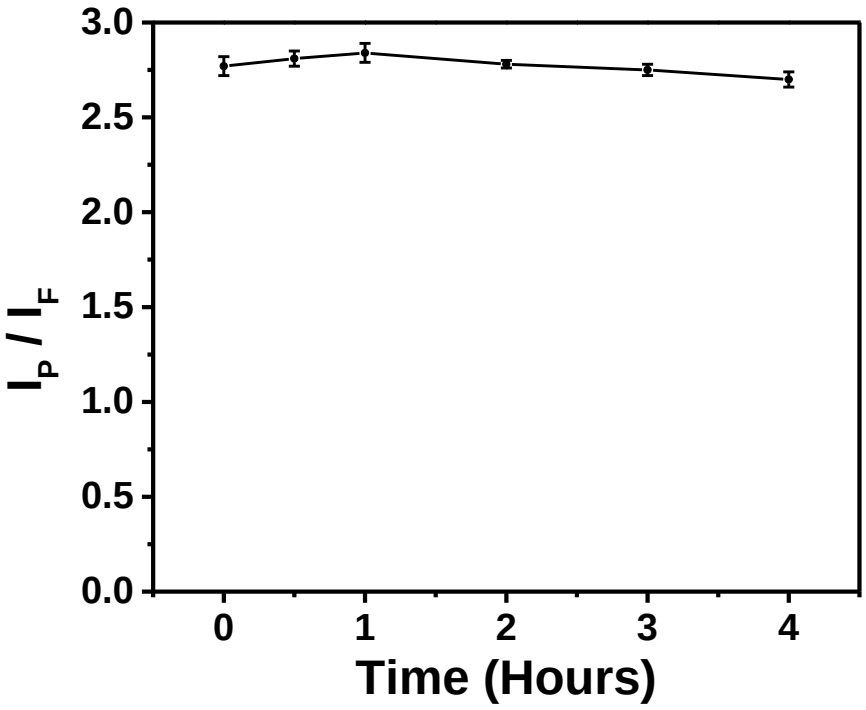

Figure S20. Time-lapse phosphorescence/fluorescence ratio of R-UiO-2 in CT26 cells in air on CLSM.

12. References

1. Lu, K.; He, C.; Lin, W., Nanoscale Metal–Organic Framework for Highly Effective Photodynamic Therapy of Resistant Head and Neck Cancer. *Journal of the American Chemical Society*, 2014, 136 (48), 16712-16715.

2. D. Magde, G.E. Rojas, and P. Seybold, Solvent Dependence of the Fluorescence Lifetimes of Xanthene Dyes. *Photochem. Photobiol.*, 1999, 70, 737.